Holographically Fabricated, Highly Reflective Nanoporous Polymeric Distributed Bragg Reflectors with Red, Green, and Blue Colors

Haodong Jiang, Wenfeng Cai, Ke Li, Ming Cheng, Vineet Kumar, Zhen Yin, Davy Gérard, Dan Luo, Quanquan Mu, Yan Jun Liu

Holographically Fabricated, Highly Reflective Nanoporous Polymeric Distributed Bragg Reflectors with Red, Green, and Blue Colors

Haodong Jiang,[1,2] Wengfeng Cai,[1] Ke Li,[1,3] Ming Cheng,[1] Vineet Kumar,[1] Zhen Yin,[1] Davy Gérard,[3] Dan Luo,[1] Quanquan Mu,[4] and Yan Jun Liu[1,4,5,*]

[1]*Department of Electrical and Electronic Engineering, Southern University of Science and Technology, Shenzhen 518055, China*

[2]*Harbin Institute of Technology, Harbin 150001, China*

[3]*Light, nanomaterials, nanotechnologies (L2n), Université de Technologie de Troyes & CNRS ERL 7004, 10004 Troyes, France*

[4]*State Key Laboratory of Applied Optics, Changchun Institute of Optics, Fine Mechanics and Physics, Chinese Academy of Sciences, Changchun 130033, China*

[5]*Key Laboratory of Energy Conversion and Storage Technologies (Southern University of Science and Technology), Ministry of Education, Shenzhen 518055, China*

**Corresponding author*: yjliu@sustech.edu.cn

Abstract: We report holographic fabrication of nanoporous distributed Bragg reflector (DBR) films with periodic nanoscale porosity via a single-prism configuration. The nanoporous DBR films result from the phase separation in a material recipe, which consists of a polymerizable acrylate monomer and nonreactive volatile solvent. By changing the interfering angle of two laser beams, we achieve the nanoporous DBR films with highly reflective RGB colors. The reflection band of the nanoporous DBR films can be tuned by further filling different liquids into the pores inside the films, resulting in the color change accordingly. Experimental results show that such kind of nanoporous DBR films could be potentially useful for many applications, such as color filters and refractive index sensors.

Keywords: distributed Bragg reflector, nanoporous reflection grating, holographic fabrication, phase separation, refractive index sensing

A distributed Bragg reflector (DBR) [1] is a periodic structure formed from alternating dielectric layers that can be used to achieve near unit reflectance within a range of frequencies. By designing DBR films with different periods and refractive indices, one can selectively achieve reflection or transmission of specific wavelength of light [2]. In the past decades, the DBR films have been widely used in sensors [3], displays [4], lasers [5], LEDs [6] and other optoelectronic devices [7,8]. Thus far, the DBR films are typically fabricated via evaporation and coating techniques, such as physical/chemical deposition, spin-coating, Langmuir-Blodgett coating, etc. However, these techniques usually require complicated multi-step processes, long fabrication time, or costly facilities, hence limiting further development of DBR applications. Therefore, it is highly desired to develop a simple, fast and cost-effective technique to fabricate the DBR films.

Along this line, the laser holographic technique could be the best option since it provides a single-step and rapid fabrication process for highly ordered structures. A typical holographic process starts with a photopolymerizable prepolymer material. Upon holographic exposure, the cured photopolymer gives rise to periodic index modulations that are governed by the interference pattern of coherent laser beams [9,10]. Depending on the interference configurations, one-, two-, or three-dimensional (1D, 2D or 3D) periodic structures can be created. By adding the nonreactive liquid crystals (LCs) into the prepolymer mixture, one can therefore achieve the ordered polymer-LC structures with tunable optical properties, resulting in many useful photonic applications [11−19]. This LC-involving patterning process is widely known as the holographic polymer-dispersed liquid crystal (HPDLC) technique [20,21]. Similarly, the addition of other additives such as nanoparticles into these holographic formulations has been also investigated [22–24]. Simultaneous addition of LCs and nanoparticles in the HPDLC formulation is expected to achieve the ordered structures with enhanced optical properties [25–27].

The 1D HPDLC periodic structures (i.e., gratings) are natural DBRs [28–34], which have been extensively investigated for many applications [35–38]. Particularly, the

1D HPDLC reflection gratings have long been studied for optical filters and reflective displays [32]. For the grating fabrication, the nature of coherent light illumination and the viscosity of the prepolymer syrup affect the phase separation of LC and polymer significantly during the photopolymerization process. Usually, upon the LCs partially separate from the polymer, numerous optically anisotropic LC droplets are formed, which will further cause nonnegligible light scattering. As a result, the strong light scattering could kill the phase separation due to polymerization in patterned periodic fashion [39–41], leading to formation of a poor-quality grating. This effect can be greatly suppressed by elevating the polymerization temperature above the clearing point of LCs. The elevated temperature decreases not only the anisotropy effect of LCs, but also the viscosity of the prepolymer syrup that greatly facilitate the phase separation [39,40]. Another possible way is to add the nonreactive additive. Hsiao and coworkers have reported porous reflection gratings fabricated from an acetone-added HPDLC formulation using visible laser (wavelength: 514 nm) holography [42–44]. Applications including humidity sensors have been also demonstrated [45–47]. However, only red-color reflection grating can be achieved at the normal incidence using the visible laser holography technique. In addition, the reflectance of nanoporous DBRs is still not high enough and the reflection band is a bit wide due to the strong scattering, which greatly limits their further applications.

In this work, we report highly reflective nanoporous DBRs with a modified HPDLC formulation via a single-prism-based ultraviolet (UV) interference setup. By changing the interference angle, nanoporous DBRs with three primary colors (red, green, and blue) are achieved after the removal of LCs. Such a kind of nanoporous DBRs is potentially useful for various applications including sensors, filters, holograms, etc.

In our experiments, the prepolymer syrup consists of 30 wt% nematic liquid crystal E7 (Jiangsu Hecheng Display Co., Ltd.), 40 wt% reactive mixture, and 30 wt% volatile solvent, acetone (Shanghai Lingfeng Chemical Reagent Co., Ltd.). The reactive mixture consists of 35 wt% monomer, Trimethylolpropane triacrylate (TMPTA, Aldrich), 3 wt% cross-linking monomer, RM257 (Shijiazhuang Stiano Fine

Chemical Co., Ltd.), 1 wt% UV photoinitiator 1173 (2-Hydroxy-2-methylpropiophenone, Aldrich), 1 wt% co-initiator, N-Phenylglycine (NPG, Aldrich).

All the materials were homogeneously mixed at 45 °C by stirring at 1000 rad/s for 2 hours. Then we added acetone into the mixture. A LC cell was assembled with two pieces of cleaned soda glass (size: 4 × 4 cm^2) using the optical adhesive NOA65. The cell gap was controlled to be 10 μm using the SiO_2 ball spacers. The prepolymer syrup was then injected into the LC cell via the capillary action.

The reflection spectra of nanoporous DBR films were measured using a UV–Vis–NIR microspectrophotometer (CRAIC 20/30 PV™) with a 75W broadband Xenon light source. The probe light beam was focused to have a detecting area of 15 × 15 μm^2 using a 36× objective lens combined with a variable aperture. The morphologies of nanoporous DBR films were investigated by the field emission scanning electron microscopy (FESEM, Merlin, Zeiss) at an acceleration voltage of 5 kV. For refractive index sensing test, four solvents with different refractive indices were used. They were methanol (n_m = 1.328), ethanol (n_e = 1.361), n-propanol (n_p = 1.384), n-butanol (n_b = 1.399), respectively.

The experimental setup of the single-prism-based holography system is schematically illustrated in Fig. 1a. An Ar^+ laser (Model: Innova 306C, Wavelength: 363.6 nm, Coherent, USA) was used as the light source. The output laser beam was subsequentially filtered, expanded, and then collimated with a beam size of 2 cm in diameter. The collimated laser beam was then impinged on a designed prism. At a certain incident angle, total internal reflection took place for the incident laser beam at the glass-air interface of the prism. As a result, the incident beam and its own total internally reflected one interfered each other and formed a periodic interference pattern. The designed prism is made of quartz and has its apex angle of α = 64° with a purpose to achieve the red-color nanoporous DBR films and have the ease of adjusting the incident angle as well. A LC cell filled with the prepolymer syrup was in optical contact with the base of the prism using an index-matching oil to further form

the interference pattern inside the cell. Fig. 1b shows the specific optical path of laser in the prism and LC cell. With the help of the matching oil, the laser beam entered the LC cell and totally reflected at the glass-air interface. The prism was placed on a rotation stage for the ease of changing the incident angle θ of the collimated laser beam. By doing so, the period of the interference pattern can be conveniently changed. As a result, we can achieve the polymeric DBR films with different periods. All the experiments were carried out at room temperature.

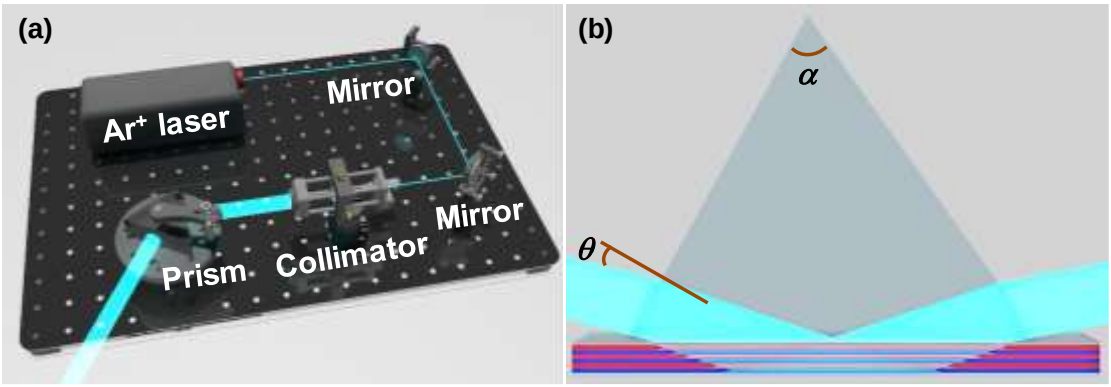

Figure 1. (a) Experimental setup for fabricating DBR films. (b) Schematic optical interference inside the LC cell via the single-prism configuration.

To estimate the period of the interference pattern, we have carried out the simulation of the laser interference based on the prism using the finite-difference time-domain (FDTD) method. The wavelength of a monochromatic light source was set to be 364 nm. The refractive index of the prism is 1.47. In our simulation, we have set three different incident angles of 7°, 14°, and 21°, respectively. The simulation results were shown in Fig. 2. It is obvious that the period of the interference pattern becomes large as the incident angle increases. The simulated periods at the three incident angles were ~350 nm, ~450 nm, and ~650 nm, respectively. From the simulation results, we can therefore carry out the experiments for the fabrication of DBR films.

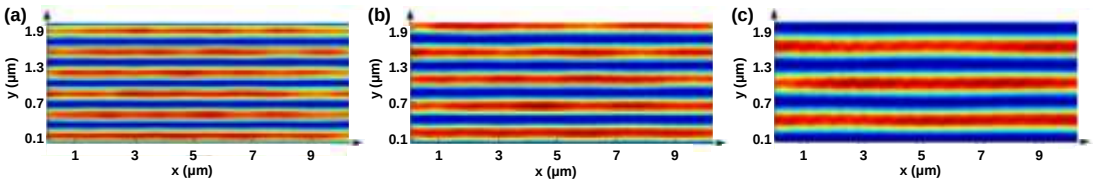

Figure 2. Simulated interference patterns with three different incident angles of (a) 7°, (b) 14°, and (c) 21°, respectively.

Upon exposure to the interference patterning with the beam intensity of 10 mW/cm^2 for 2 min, the LC cells were then exposed to the UV light for ~30 mins with the exposure intensity of 10 mW/cm^2 and then post-cured for 24 hr in air to ensure the complete polymerization. Upon opening the LC cell to separate the cured sample from one cover slide, the acetone inside the cured sample will evaporate rapidly and a nanoporous polymeric DBR film situated on the other cover slide was then achieved. It is worth mentioning that when the cell was opened, the DBR films tended to situate on the cover slide that was nearest to the incoming light. We noticed that there was a big difference on the appearance of the sample before and after the cell opening. The sealed LC cells after the UV laser exposure demonstrate a totally transparent state, as shown in Fig. 3a$_1$ and 3a$_2$. The total transparency can be mainly attributed to the index matching due to the presence of isotropic solvent (i.e., acetone). However, the nanoporous polymeric DBR film presents a translucent state (see Fig. 3b$_1$ and 3b$_2$). The evaporation of acetone leads to numerous air nanopores inside the polymers, which further cause strong scattering, making the DBR film opaque. Fig. 3a$_3$ and 3a$_3$ shows the measured transmission and reflection spectra of the three samples before and after the cell opening. From Fig. 3a$_3$, it is obvious that the three samples before the cell opening have quite high transmittance (near 80%) and reflectance (near 20%) across the whole visible range. In contrast, after the cell opening, there is significant decrease of the transmission and slight decrease of the reflection, as shown in Fig. 3b$_3$. Moreover, When the acetone evaporated after the cell opening, air nanopores were created. Meanwhile, the formed liquid crystal nanodroplets were still left inside the polymer matrix. These air nanopores and LC nanodroplets will create a slightly larger index modulation within the film compared to the originally acetone and LC nanodroplets. As a result, upon the acetone evaporation, clearly observable peaks/dips appeared on the measured refection/transmission spectra for blue and green films. It is worth mentioning that we used different references in our spectral measurement. For transmittance measurement, we used the free-space light transmission in air as the reference, while for reflectance measurement, we used an Ag mirror as the reference.

Since the Ag mirror doesn't have 100% reflection, the measured reflection of the DBR films will be higher than the theoretical prediction. As a result, we observed relatively high reflectance.

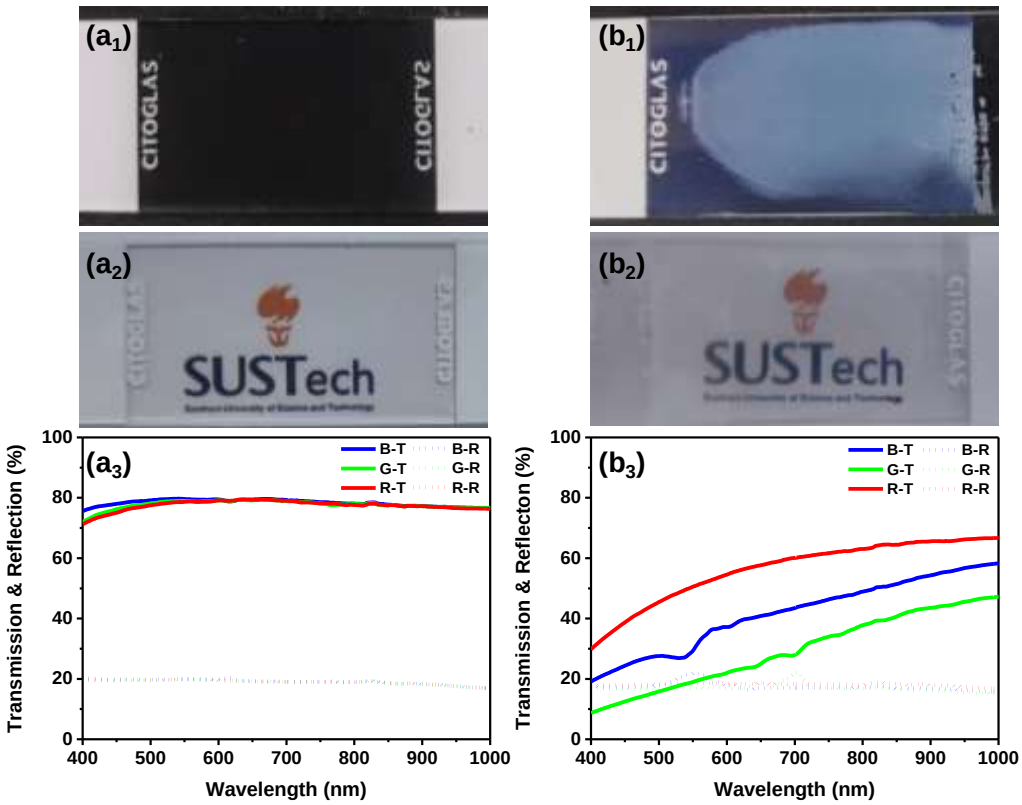

Figure 3. Transparency-tested photos for a blue film before (a_1 and a_2) and after (b_1 and b_2) the cell opening, which were taken from the black (a_1 and b_1) and white (a_2 and b_2) backgrounds, respectively. Measured transmission and reflection spectra for blue, green and red films before (a_3) and after (b_3) the cell opening, respectively.

We have to mention that although the acetone evaporated after the LC cell was opened, the LCs were still left inside the films. To further remove the LCs trapped inside the films, we used the ethanol to wash away the LCs. When the LC nanodroplets were washed away, complete air nanopores were created, resulting in a much larger index modulation. Therefore, after the removal of LCs, the nanoporous polymeric DBR films demonstrate a colored appearance. In our experiments, at three different incident angles of 7°, 14° and 21°, we have achieved blue, green and red colored DBR films, respectively, as shown in Fig. 4a_1&a_2, b_1&b_2 and c_1&c_2. We can clearly see the shiny blue, green and red colors both macroscopically and microscopically from the samples. It is worth mentioning that a macroscopic look at

DBR films shows nonuniform colors with fingerprint-like patterns, which could be mainly attributed to the nonuniform thickness of the index-matching oil in the optical contact. By accurately controlling the uniform thickness of the index-matching oil, this fingerprint-like pattern could be completely avoided, and hence a uniform color can be achieved accordingly.

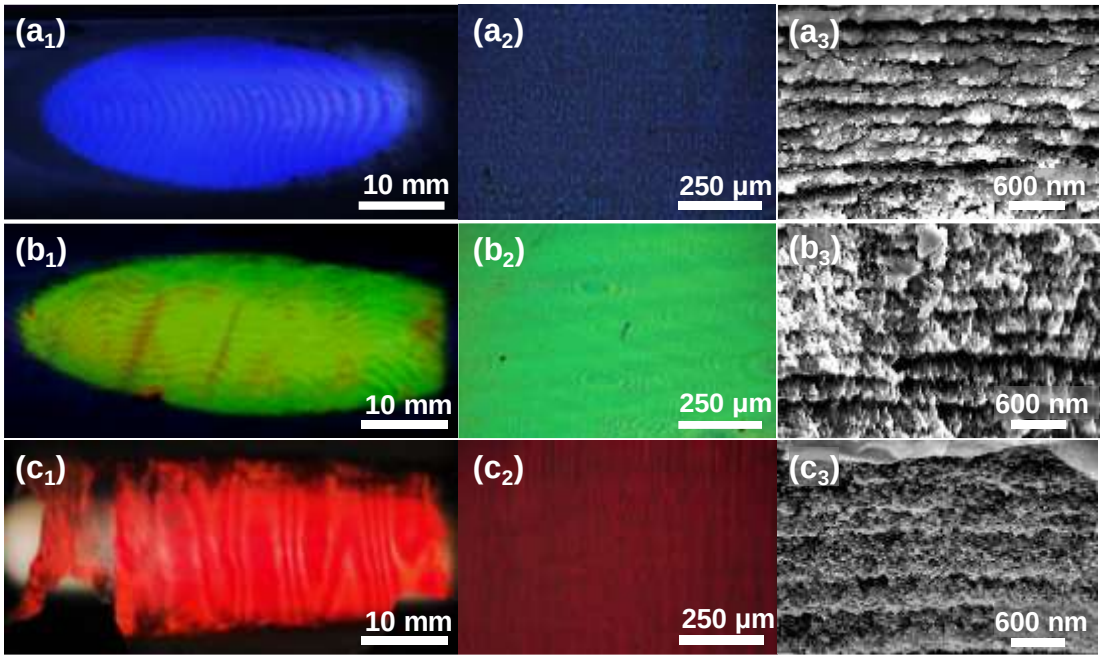

Figure 4. Camera photos (a_1, b_1 and c_1), optical microscopic images (a_2, b_2 and c_2), SEM images (a_3, b_3 and c_3) of the blue (a_1–a_3), green (b_1–b_3), and red (c_1–d_3) films, respectively.

To further check the morphological details of the DBR films, we have carried out the SEM investigation on three colored samples. Fig. 3a_3–c_3 shows the typically observed cross-sectional SEM images that reflect the detailed morphologies of the nanoporous polymeric DBR films. It can be clearly seen that the films have a multi-layered structure that consists of alternative polymer-rich and nanopore-rich layers. Therefore, they can highly reflect a certain wavelength range of the light. We can also see that as the reflection color changes from blue to red, the period of the DBR films increases gradually. The measured periods of the blue, green and red films are ~350, ~458, and ~663 nm, respectively. A close look at the morphologies reveals that the nanopore diameters range from a few nanometers to tens of nanometers, and the porosity of the polymeric DBR structure is in a range of 20–40%.

As mentioned, the observed visible colors originate from the high reflection of the nanoporous DBR films. The reflection spectra of the films were therefore measured using a UV–Vis–NIR microspectrophotometer. Fig. 5 shows the measured reflection spectra for the blue, green and red samples, respectively. The red and green films have the reflection of larger than 90%, while the blue one has comparatively low reflectance but still higher than 70%. The relatively low reflection for the blue film is mainly attributed to the slightly high absorption of the polymer materials at the blue range. In addition, we can also see from Fig. 5 that the full-width at half-maximum (FWHM) gradually decreases as the reflection band shifts from blue to red. The FWHM of the reflection bands are 46, 42, and 30 nm for blue, green, and red films, respectively. The larger FWHM for the blue film might be caused by the nanopore-induced relatively stronger scattering in the blue range. As the light wavelength in the red range becomes larger, the nanopore-induced scattering becomes weak, hence resulting in a smaller FWHM.

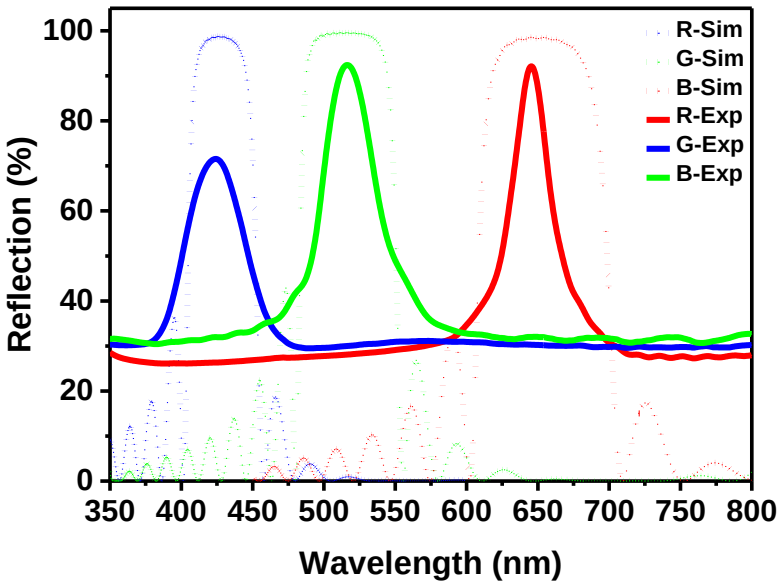

Figure 5. Measured and simulated reflection spectra for the blue, green, and red films, respectively.

Based on the Bragg condition, color of the reflected film is dependent on the periodic fringe formed by the laser interference. Hence, we have theoretically calculated the reflection curves. The refractive indices of polymer matrices and air were assumed to be 1.47 and 1, respectively. The DBR films were all assumed to have 10 pairs of

polymer-rich and nanopore-rich layers. The other data used in our calculations were tabulated in Table 1. It is worth mentioning that in our calculations, the wavelength dispersion of the refractive indices of the composed materials is not considered because their refractive index changes in the visible range are small enough to be ignored. We have also taken into account the shrinkage of 10–20% of the polymerization and nanopores due to the evaporation of the solvents. It is evident that the calculated curves are in reasonable agreement with the measured ones.

Table 1. The estimated thickness of the polymer-rich and nanopore-rich layers for the blue, green and red films.

Sample	Total Period (nm)	Polymer Layer (nm)	Air Layer (nm)
Blue	350	204	146
Green	458	237	221
Red	663	319	344

In principle, the reflection band of the nanoporous polymeric DBR films is mainly determined by their filling ratio and refractive index contrast between the polymer-rich and nanopore-rich layers at the fixed period. It is quite straightforward that the reflection band will be shifted when the air nanopores are filled with other materials that have different refractive indices. Therefore, the achieved nanoporous polymeric DBRs are potentially useful for optical sensing applications. In this regard, we carried out a refractive index sensing test using our nanoporous polymeric DBRs. We have investigated the changes of the reflection spectra for the blue, green and red films that infiltrated with four different solvents. The measured spectral changes are shown in Fig. 6. Overall, the measured reflection spectra for these three colored DBR films show a similar trend after the filling with the four liquids. As the refractive index increases, the reflection peak shows an obvious redshift for each film. In addition, the reflection peak intensity decreases as well. Fig. 6d summarizes the peak and intensity change as the function of the refractive index. A linear change can be well observed for the blue and green films. There is slight variation for the red one as the reflection peak becomes low and broad, causing that the measurement is not accurate enough.

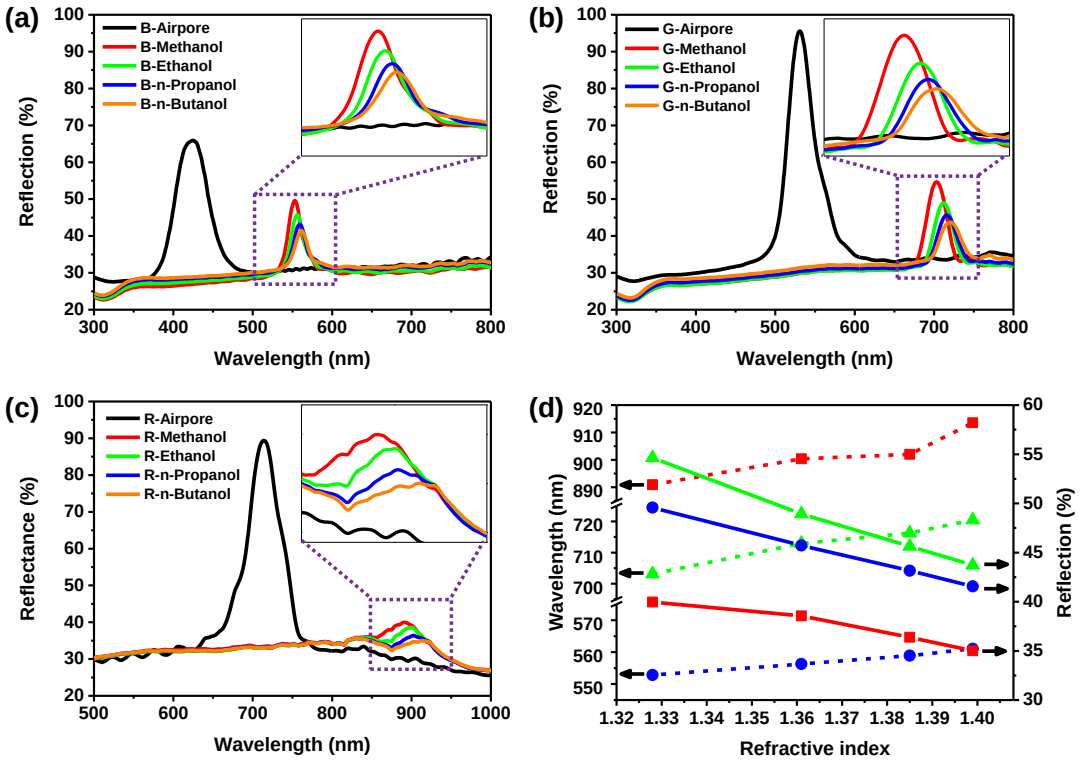

Figure 6. Measured spectral changes of the reflection for the blue (a), green (b), and red (c) films that infiltrated with methanol, ethanol, n-propanol, and n-butanol, respectively. (d) Summarized peak and intensity change as the function of the refractive index.

Using the Bragg's Law, the center wavelength of the reflection spectrum can be determined by [43]

$$\lambda_{\text{Bragg}} = 2\left(n_1 d_1 + n_2 d_2\right) \tag{1}$$

where for our case, n_1 and d_1 are the refractive index and thickness of the polymeric layer, n_2 and d_2 are the refractive index and thickness of the nanoporous layer. For the refractive index sensing test, the refractive index change of the nanoporous layer (i.e., n_2) plays a dominant role. When n_2 increases, the reflected center wavelength increases as well. As a result, we observed a clear redshift of the reflection peak. On the other hand, in the extreme case, when n_2 increases to be equal to n_1 (i.e., reach the complete index matching condition), the DBR film will become totally transparent. There is no reflection caused by the index mismatch between the polymer-rich and nanopore-rich layers. Therefore, we also observed the intensity decrease of the reflection peak.

In summary, we have demonstrated nanoporous polymeric DBR films with periodic nanoscale porosity via a single-prism holography technique. The nanoporous DBR films consisted of alternative polymer-rich and air-nanopore-rich layers. By changing the interfering angle of two laser beams, we have achieved highly reflective nanoporous DBR films with red, green, and blue colors. Their reflectance can be larger than 70% for blue, and 90% for green and red wavelength range. We have also experimentally confirmed that the reflection band of the nanoporous DBR films can be deliberately tuned by further filling different solvents into the pores inside the films, indicating that they are highly sensitive to the refractive index. Such kind of nanoporous polymeric DBR films could be potentially useful for many applications, such as color filters and refractive index sensors.

Acknowledgements

This work was supported in part by National Natural Science Foundation of China (Grant No. 61805113), Natural Science Foundation of Guangdong Province (Grant No. 2017A030313034 and 2018A030310224), Shenzhen Science and Technology Innovation Commission (Grant No. JCYJ20180305180635082, JCYJ20170817111349280, and GJHZ20180928155207206), Open Fund of State Key Laboratory of Applied Optics (Grant No. SKLAO-201904), and Guangdong Innovative and Entrepreneurial Research Team Program (Grant No. 2017ZT07C071). We acknowledge the help and discussion from Prof. Vincent Hisao at Taiwan Chi Nan University. The authors also acknowledge the assistance of SUSTech Core Research Facilities.

References

1 P. Lova, G. Manfredi, and D. Comoretto, "Advances in functional solution processed planar 1D photonic crystals", Adv. Opt. Mater. **6**, 1800730 (2018).

2 D. P. Puzzo, L. D. Bonifacio, J. Oreopoulos, C. M. Yip, I. Manners, and G. A. Ozin, "Color from colorless nanomaterials: Bragg reflectors made of nanoparticles", J. Mater. Chem. **19**, 3500–3506 (2009).

3 D. Kersey, M. A. Davis, H. J. Patrick, M. LeBlanc, K. Koo, C. Askins, M. Putnam, and E. J. Friebele, "Fiber grating sensors", J. Lightwave Technol. **15**,

1442–1463 (1997).

4 K.-J. Chen, H.-C. Chen, K.-A. Tsai, C.-C. Lin, H.-H. Tsai, S.-H. Chien, B.-S. Cheng, Y.-J. Hsu, M.-H. Shih, C.-H. Tsai, H.-H. Shih, and H.-C. Kuo, "Resonant-enhanced full-color emission of quantum-dot-based display technology using a pulsed spray method", Adv. Funct. Mater. **22**, 5138–5143 (2012).

5 V. Jayaraman, Z.-M. Chuang, and L. A. Coldren, "Theory, design, and performance of extended tuning range semiconductor lasers with sampled gratings", IEEE J. Quant. Electron. **29**, 1824–1834 (1993).

6 K. Neyts, P. De Visschere, D. K. Fork, and G. B. Anderson, "Semitransparent metal or distributed Bragg reflector for wide-viewing-angle organic light-emitting-diode microcavities", J. Opt. Soc. Am. B **17**, 114–119 (2000).

7 Shelykh, M. Kaliteevskii, A. Kavokin, S. Brand, R. Abram, J. Chamberlain, and G. Malpuech, "Interface photonic states at the boundary between a metal and a dielectric Bragg mirror", Phys. Status Solidi A **204**, 522–525 (2007).

8 S. Brand, M. Kaliteevski, and R. Abram, "Optical Tamm states above the bulk plasma frequency at a Bragg stack/metal interface", Phys. Rev. B **79**, 085416 (2009).

9 Y. J. Liu, H. T. Dai, and X. W. Sun, "Holographic fabrication of azo-dye-functionalized photonic structures", J. Mater. Chem. **21**, 2982–2986 (2011).

10 Y. J. Liu, H. T. Dai, E. S. P. Leong, J. H. Teng, and X. W. Sun, "Azo-dye-doped absorbing photonic crystals with purely imaginary refractive index contrast and all-optically switchable diffraction properties", Opt. Mater. Express **2**, 55–61 (2012).

11 V. P. Tondiglia, L. V. Natarajan, R. L. Sutherland, D. Tomlin, and T. J. Bunning, "Holographic formation of electro-optical polymer-liquid crystal photonic crystals", Adv. Mater. **14**, 187–191 (2002).

12 M. J. Escuti and G. P. Crawford, "Holographic photonic crystals", Opt. Eng. **43**, 1973–1987 (2004).

13 Y. J. Liu and X. W. Sun, "Electrically tunable two-dimensional holographic photonic crystals fabricated by a single diffractive element", Appl. Phys. Lett. 89, 171101 (2006).

14 Y. J. Liu and X. W. Sun, "Electrically tunable three-dimensional holographic photonic crystals made of polymer-dispersed liquid crystal", Jpn. J. Appl. Phys. **46**, 6634–6638 (2007).

15 Z. Zheng, J. Song, Y. Liu, F. Guo, J. Ma, and L. Xuan, "Single-step exposure for two-dimensional electrically-tuneable diffraction grating based on polymer dispersed liquid crystal", Liq. Cryst. **35**, 489–499 (2008).

16 J. Zheng, G. Sun, K. Wen, T. Wang, S. Zhuang, Y. Liu, and S. Yin, "Electrically controlled optical choppers based on holographic polymer dispersed liquid crystal gratings", Chin. Opt. Lett. **8**, 1167–1170 (2010).

17 G. Chen, M. Ni, H. Peng, F. Huang, Y. Liao, M. Wang, J. Zhu, V. A. L. Roy, and X. Xie, "Photoinitiation and inhibition under monochromatic green light for storage of colored 3D images in holographic polymer-dispersed liquid crystals", ACS Appl. Mater. Interfaces **9**, 1810–1819 (2017).

18 Y. Zhao, X. Zhao, M.-D. Li, Z. Li, H. Peng, and X. Xie, "Crosstalk-free patterning of cooperative-thermoresponse images by the synergy of the AIEgen with the liquid crystal", Angew. Chem. Int. Ed. **59**, 10066–10072 (2020).

19 W.-C. Luo, Y.-D. Xu, G.-X. Yu, S.-S. Li, H.-Y. Li, and L.-J. Chen, "Reconfigurable polymer-templated liquid crystal holographic gratings via visible-light recording", Opt. Express **28**, 17307–17319 (2020).

20 T. J. Bunning, L. V. Natarajan, V. P. Tondiglia, and R. L. Sutherland, "Holographic polymer-dispersed liquid crystals (H-PDLCs)", Annu. Rev. Mater. Sci. **30**, 83–115 (2000).

21 Y. J. Liu and X. W. Sun, "Holographic polymer-dispersed liquid crystals: Materials, formation, and applications", Adv. Optoelectron. **2008**, 684349 (2008).

22 Y. Tomita, N. Suzuki, and K. Chikama, "Holographic manipulation of nanoparticle distribution morphology in nanoparticle-dispersed photopolymers", Opt. Lett. **30**, 839–841 (2005).

23 V. Pramitha, K. P. Nimmi, N. V. Subramanyan, R. Joseph, K. Sreekumar, and C. S. Kartha, "Silver-doped photopolymer media for holographic recording", Appl. Opt. **48**, 2255–2261 (2009).

24 C. Li, L. Cao, Q. He, and G. Jin, "Holographic kinetics for mixed volume gratings in gold nanoparticles doped photopolymer", Opt. Express **22**, 5017–5028 (2014).

25 A. Hinojosa and S. C. Sharma, "Effects of gold nanoparticles on electro-optical properties of a polymer-dispersed liquid crystal", Appl. Phys. Lett. **97**, 081114 (2010).

26 M. Zhang, J. Zheng, K. Gui, K. Wang, C. Guo, X. Wei, and S. Zhuang, "Electro-optical characteristics of holographic polymer dispersed liquid crystal gratings doped with nanosilver", Appl. Opt. **52**, 7411–7418 (2013).

27 Y. Liu, J. Zheng, T. Shen, K. Wang, and S. Zhuang, "Diffusion kinetics investigations of Nano Ag-doped holographic polymer dispersed liquid crystal gratings", Liq. Cryst. **46**, 1852–1860 (2019).

28 R. L. Sutherland, L. V. Natarajan, V. P. Tondiglia, and T. J. Bunning, "Bragg gratings in an acrylate polymer consisting of periodic polymer-dispersed liquid-crystal planes", Chem. Mater. **5**, 1533–1538 (1993).

29 R. Caputo, L. De Sio, A. Veltri, C. Umeton, and A. V. Sukhov, "Development of a new kind of switchable holographic grating made of liquid-crystal films separated by slices of polymeric material", Opt. Lett. **29**, 1261–1263 (2004).

30 Y. J. Liu, X. W. Sun, J. H. Liu, H. T. Dai, and K. S. Xu, "A polarization insensitive 2×2 optical switch fabricated by liquid crystal-polymer composites", Appl. Phys. Lett. **86**, 041115 (2005).

31 Y. J. Liu, Y. B. Zheng, J. Shi, H. Huang, T. R. Walker, and T. J. Huang, "Optically switchable gratings based on azo-dye-doped, polymer-dispersed liquid crystals", Opt. Lett. **34**, 2351–2353 (2009).

32 H. Yuan, J. Colegrove, G. Hu, T. Fiske, A. Lewis, J. Gunther, L. Silverstein, C. Bowley, G. Grawford, L. Chien, and J. Kelly, "HPDLC color reflective displays", SPIE **3690**, 196–206 (1999).

33 L.V. Natarajan, C. K. Shepherd, D. M. Brandelik, R. L. Sutherland, S. Chandra, V. P. Tondiglia, D. Tomlin, and T. J. Bunning, "Switchable holographic polymer-dispersed liquid crystal reflection gratings based on thiol-ene photopolymerization", Chem. Mater. **15**, 2477–2484 (2003).

34 M. S. Park, B. K. Kim, and J. C. Kim, "Reflective mode of HPDLC with various structures of polyurethane acrylates", Polymer **44**, 1595–1602 (2003).

35 R. Jakubiak, L. V. Natarajan, V. Tondiglia, G. S. He, P. N. Prasad, T. J. Bunning, and R. A. Vaia, "Electrically switchable lasing from pyrromethene 597 embedded holographic-polymer dispersed liquid crystals", Appl. Phys. Lett. **85**, 6095–6097 (2004).

36 V. K.S. Hsiao, C. Lu, G. S. He, M. Pan, A. N. Cartwright, P. N. Prasad, R. Jakubiak, R. A. Vaia, and T. J. Bunning, "High contrast switching of distributed-feedback lasing in dye-doped H-PDLC transmission grating structures", Opt. Express **13**, 3787–3794 (2005)

37 Y. J. Liu, X. W. Sun, P. Shum, H. P. Li, J. Mi, W. Ji, and X. H. Zhang, "Low-threshold and narrow-linewidth lasing from dye-doped holographic polymer-dispersed liquid crystal transmission gratings", Appl. Phys. Lett. **88**, 061107 (2006).

38 Y. J. Liu, X. W. Sun, H. I. Elim, and W. Ji, "Effect of liquid crystal concentration on the lasing properties of dye-doped holographic polymer-dispersed liquid crystal transmission gratings", Appl. Phys. Lett. **90**, 011109 (2007).

39 Y. J. Liu, B. Zhang, Y. Jia, and K. S. Xu, "Improvement of the diffraction properties in holographic polymer dispersed liquid crystal Bragg gratings", Opt. Commun. **218**, 27–32 (2003).

40 R. Caputo, A. Veltri, C. P. Umeton, and A. V. Sukhov, "Characterization of the diffraction efficiency of new holographic gratings with a nematic film–polymer-slice sequence structure", J. Opt. Soc. Am. B **21**, 1939–1947 (2004).

41 Y. J. Liu, X. W. Sun, H. T. Dai, J. H. Liu, and K. S. Xu, "Effect of surfactant on the electro-optical properties of holographic polymer dispersed liquid crystal Bragg gratings", Opt. Mater. **27**, 1451–1455 (2005).

42 V. K. S. Hsiao, T.-C. Lin, G. S. He, A. N. Cartwright, P. N. Prasad, L. V. Natarajan, V. P. Tondiglia, and T. J. Bunning, "Optical microfabrication of highly reflective volume Bragg gratings", Appl. Phys. Lett. **86**, 131113 (2005).

43 V. K. S. Hsiao, K.-T. Yong, A. N. Cartwright, M. T. Swihart, P. N. Prasad, P. F. Lloyd, and T. J. Bunning, "Nanoporous polymeric photonic crystals by emulsion holography", J. Mater. Chem. **19**, 3998–4003 (2009).

44 V. K. S. Hsiao, T. J. White, A. N. Cartwright, P. N. Prasad, and C. A. Guymon, "Influence of non-reactive solvent on optical performance, photopolymerization kinetics and morphology of nanoporous polymer gratings", Eur. Polym. J. **46**, 937–943 (2010).

45 V. K. S. Hsiao, W. D. Kirkey, F. Chen, A. N. Cartwright, P. N. Prasad, and T. J. Bunning, "Organic solvent vapor detection using holographic photopolymer reflection gratings", Adv. Mater. **17**, 2211–2214 (2005).

46 J. Shi, V. K. S. Hsiao, and T. J. Huang, "Nanoporous polymeric transmission gratings for high-speed humidity sensing", Nanotechnology **18**, 465501 (2007).

47 J. Shi, V. K. S. Hsiao, T. R. Walker, and T. J. Huang, "Humidity sensing based on nanoporous polymeric photonic crystals", Sens. Actuators B: Chem. **129**, 391–396 (2008).